A Deterministic Filter for Simultaneous Localization and Odometry Calibration of Differential-Drive Mobile Robots

Gianluca Antonelli* Stefano Chiaverini*
*Dipartimento di Automazione, Elettromagnetismo,
Ingegneria dell'Informazione e Matematica Industriale
Università degli Studi di Cassino
via G. Di Biasio 43, 03043 Cassino (FR), Italy.
{antonelli,chiaverini}@unicas.it
http://webuser.unicas.it/lai/robotica

***Abstract*— Local reconstruction of differential-drive mobile robots position and orientation is made possible with an accurate odometry calibration. Starting from the encoders readings, and assuming an absolute measurement available, a deterministic filter to localize the vehicle while estimating a proper set of odometric parameters is proposed. A stability analysis guarantees that the position and orientation error decreases to zero and the estimation error of the odometric parameters is bounded. The proposed technique has been experimentally validated on a Khepera II mobile robot and compared to an Extended Kalman Filter approach. With both approaches the errors are practically the same, the proposed approach, thus, represents a computationally lighter alternative to Kalman approaches with a rigorous stability analysis.**

***Index Terms*— Odometry, Calibration, Mobile Robots**

I. Introduction

The position and orientation of a mobile robot can be reconstructed starting from the odometry, i.e., resorting to the encoders' measurements at the wheels properly integrated over time. This estimation is affected mainly by threes sources of errors: numerical drift, inherently related to discrete-time integration; the presence of non-systematic errors, such as those due to wheel slippage and the presence of systematic errors, i.e., errors in the estimation of the parameters involved in the kinematics equation used to convert the readings at the wheels into data expressing the robot movement. The estimation of the odometric parameters is known in the literature as odometry calibration.

Notice that the overall error in reconstructing the vehicle's absolute configuration, i.e., its position and orientation, is often significant after a short path executed by the robot; in fact, it has been demonstrated by [10], [11] that this error shows a square dependence with the distance travelled. This is true even for robot whose odometric parameters were accurately estimated. One of the first works that focuses on odometric errors is [17], where knowledge of the path under execution is used to improve posture estimation between odometric updates. The paper by [6] performs identification of the odometric parameters based on absolute position measurements after the execution of a set of suitably defined trajectories. Reference [8] proposes to drive the robot through a known path and then evaluate the shape of the resulting path to estimate the model parameters.

In case it is possible, however, it is convenient to resort to external sensing device that provide an absolute measurement. In this case, an accurate odometric calibration is useful to optimize the estimation of the robot's configuration between two successive measurements. In [13] a sensor fusion technique is proposed where, in order to improve accuracy of the robot configuration estimate, odometry is used together with direct measurement of absolute angular velocity provided by an optical-fiber gyroscope. Multisensory measurement is also exploited in [16], where a laser sensory system is used to correct on-line the odometry through a maximum-likelihood based identification technique. The work by [9] proposes the use of a gyroscope, together with the encoders, and a GPS unit in a Kalman filter approach in order to estimate the outdoor robot's configuration; another multisensory system, applied to a car-like vehicle, is presented in [5]. Reference [14] proposes the use of an Extended Kalman Filter (EKF) in order to simultaneously localize the vehicle and estimate the vehicle odometry; paper [15] extends this approach in order to include estimation of non-systematic errors. Reference [7], finally, validate the use of an EKF for a vehicle aimed at volcano exploration.

In previous work [4], the Authors presented an off-line calibration method for a proper set of odometric parameters. The novelty of the proposed method relies in the observation that, for unicycle-like mobile robots, a linear relationship between the measurements and a proper set of odometric parameters (not the physical parameters) holds and thus it is possible to use the least-squares estimation to achieve the odometric calibration. In [2], [3], moreover, by using two successive least-squares operations, the actual physical parameters are

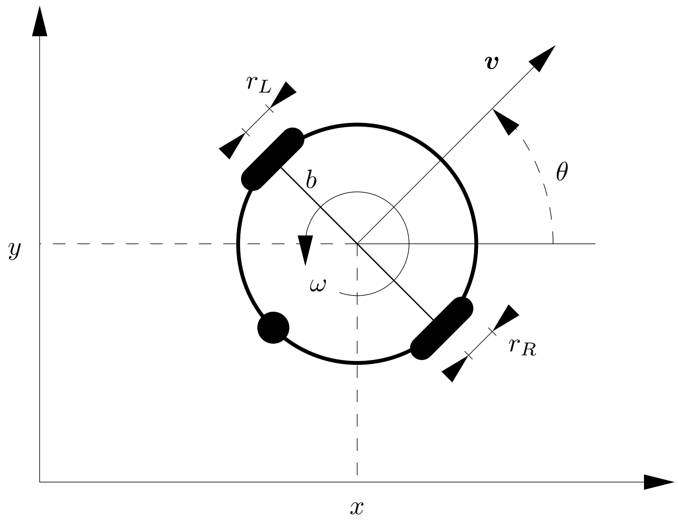

Fig. 1. Top-view sketch of a differential-drive mobile robot with relevant variables.

estimated. In both cases, no linearization is involved in the estimation. In this paper, a recursive version of [4] is proposed where both localization and parameters' estimation is achieved simultaneously. A Lyapunov-like stability analysis guarantees convergence to zero of the localization error and boundness of the parameters estimation error. This problem were solved in the literature, see, e.g., [14], by resorting to an EKF approach applied to the non-linear relationship between the physical odometric parameters and the measurements; for the latter approach, however, no formal proof of convergence exists. The proposed technique has been experimentally validated on a Khepera II mobile robot and compared to the EKF approach.

II. Modelling

Let us consider a differential-drive mobile robot as sketched in Figure 1. The motion of the left and right wheels is characterized by the sole (scalar) axis angular velocities ω_L and ω_R, respectively; the rear castor wheel is passive.

Let us consider a ground-fixed inertial reference frame Σ_i. By defining as *wheelbase* the segment of length b connecting the two lateral wheels along their common axis, it is convenient to choose a vehicle-fixed frame Σ_v such as: its origin is at the middle of the wheelbase, its x-axis points toward the front of the robot body and its y-axis points toward the left wheel, completing a right-hand frame. With this choice, the absolute velocity of the robot body can be described by the 2-dimensional vector $\boldsymbol{v}$ expressing the translational velocity of the origin of Σ_v with respect to Σ_i and by the scalar ω expressing the angular velocity of Σ_v as seen from Σ_i. A major advantage of the above choice is that, under the assumption that the wheels do not slide on the ground, the translational velocity $\boldsymbol{v}$ is always orthogonal to the wheelbase. Therefore, in the vehicle-fixed frame the vector $\boldsymbol{v}$ is completely characterized by its sole x-component denoted as v.

By denoting as x and y the coordinates of the origin of Σ_v expressed in the frame Σ_i, and as θ the heading angle between the x-axis of Σ_v and Σ_i, the robot kinematic equations are written as

$$\begin{cases} \dot{x} = v\cos(\theta) \\ \dot{y} = v\sin(\theta) \\ \dot{\theta} = \omega\,. \end{cases} \tag{1}$$

It can be recognized (see Figure 1) that the body-fixed components v and ω of the robot velocity are related to the angular velocity of the wheels by

$$\begin{cases} v = \dfrac{r_R}{2}\omega_R + \dfrac{r_L}{2}\omega_L \\ \omega = \dfrac{r_R}{b}\omega_R - \dfrac{r_L}{b}\omega_L\,. \end{cases} \tag{2}$$

in which r_R and r_L are the radiuses of the right and left wheel, respectively.

By defining as

$$\boldsymbol{p} = \begin{bmatrix} x & y & \theta \end{bmatrix}^{\mathrm{T}} \tag{3}$$

and

$$\alpha_R \;=\; \frac{r_R}{b} \tag{4}$$

$$\alpha_L \;=\; -\frac{r_L}{b}\,, \tag{5}$$

it is possible to rewrite the odometry of the vehicle as

$$\dot{\boldsymbol{p}} = \boldsymbol{\Phi}(\boldsymbol{p}, \omega_R, \omega_L)\boldsymbol{\beta} \tag{6}$$

where the vector $\boldsymbol{\beta} \in \mathbb{R}^4$ collects four odometric parameters:

$$\boldsymbol{\beta} = \begin{bmatrix} r_L & r_R & \alpha_L & \alpha_R \end{bmatrix}^{\mathrm{T}} \tag{7}$$

and the regressor $\boldsymbol{\Phi} \in \mathbb{R}^{3\times 4}$ (dependencies are dropped out to increase readability) is defined as:

$$\boldsymbol{\Phi} = \begin{bmatrix} \dfrac{1}{2}\cos(\theta)\omega_L & \dfrac{1}{2}\cos(\theta)\omega_R & 0 & 0 \\ \dfrac{1}{2}\sin(\theta)\omega_L & \dfrac{1}{2}\sin(\theta)\omega_R & 0 & 0 \\ 0 & 0 & \omega_L & \omega_R \end{bmatrix} \tag{8}$$

III. Proposed Filter

By denoting with $\hat{\boldsymbol{p}}$ and $\hat{\boldsymbol{\beta}}$ the estimated position and parameter vectors, respectively, and being

$$\tilde{\boldsymbol{p}} = \boldsymbol{p} - \hat{\boldsymbol{p}}\,, \tag{9}$$

the proposed filter is:

$$\begin{cases} \dot{\hat{\boldsymbol{p}}} = \boldsymbol{\Phi}\hat{\boldsymbol{\beta}} + \boldsymbol{K}_p\tilde{\boldsymbol{p}} \\ \dot{\hat{\boldsymbol{\beta}}} = \boldsymbol{K}_\beta\boldsymbol{\Phi}^{\mathrm{T}}\tilde{\boldsymbol{p}}\,, \end{cases} \tag{10}$$

where $\boldsymbol{K}_p \in \mathbb{R}^{3\times 3}$ and $\boldsymbol{K}_\beta \in \mathbb{R}^{4\times 4}$ are positive definite design gains. From that, the estimation of $\hat{b}$ can be obtained by resorting to (4) or (5) yielding:

$$\hat{b} = \frac{\hat{r}_R}{\hat{\alpha}_R} \qquad \text{or} \qquad \hat{b} = -\frac{\hat{r}_L}{\hat{\alpha}_L}\,. \tag{11}$$

A. Stability Analysis

Let us consider as Lyapunov function

$$V(\tilde{\boldsymbol{p}},\tilde{\boldsymbol{\beta}}) = \frac{1}{2}\tilde{\boldsymbol{p}}^{\mathrm{T}}\tilde{\boldsymbol{p}} + \frac{1}{2}\tilde{\boldsymbol{\beta}}^{\mathrm{T}}\boldsymbol{K}_{\beta}^{-1}\tilde{\boldsymbol{\beta}}, \tag{12}$$

that is clearly positive definite; its time derivative is given by

$$\dot{V}(\tilde{\boldsymbol{p}},\tilde{\boldsymbol{\beta}}) = \tilde{\boldsymbol{p}}^{\mathrm{T}}\left(\boldsymbol{\Phi}\boldsymbol{\beta} - \dot{\hat{\boldsymbol{p}}}\right) - \tilde{\boldsymbol{\beta}}^{\mathrm{T}}\boldsymbol{K}_{\beta}^{-1}\dot{\hat{\boldsymbol{\beta}}} \tag{13}$$

where the assumption that the vector of parameters $\boldsymbol{\beta}$ is constant were made. By substituting the equations (10), and after some basic computations, one easily obtains:

$$\dot{V}(\tilde{\boldsymbol{p}},\tilde{\boldsymbol{\beta}}) = -\tilde{\boldsymbol{p}}^{\mathrm{T}}\boldsymbol{K}_{p}\tilde{\boldsymbol{p}} \tag{14}$$

that is $\dot{V}(\tilde{\boldsymbol{p}},\tilde{\boldsymbol{\beta}}) \leq 0$.

Since the system is non-autonomous the stability can not be derived by applying the La Salle variant of the Lyapunov's theorem. By further assuming that $\boldsymbol{p}$ is twice differentiable, then $\ddot{V}$ is bounded and $\dot{V}$ is uniformly continuous. Moreover, since V is lower bounded, application of the Barbălat's Lemma [12] allows to prove global convergence of $\tilde{\boldsymbol{p}} \to \boldsymbol{0}$ as $t \to \infty$. Moreover, due to the filter's definition, it can be observed that $\tilde{\boldsymbol{\beta}}$ is bounded.

Concerning the odometric parameters it should be remarked that the proposed filter gives information on the vector $\hat{\boldsymbol{\beta}}$ and thus on the two intermediate variables α_R and α_L and not on the physical parameter b.

Notice that, at the best of our knowledge, with the Extended Kalman Filter no formal proof of convergence exists even for the sole position and orientation variables.

IV. Experimental Results

Experiments were run using the Khepera II mobile robot, shown in Figure 2, manufactured by K-Team [1].

The vision system used is composed by a rgb-camera that estimate the vehicle configuration by resorting to a camera-calibration procedure and image-based feature extraction. The overall configuration error can be estimated as bounded by few millimeters and few degrees [3].

The robot is equipped with a Bluetooth communication module that allows to control the vehicle and read the wheels position/velocities with a sampling time

$$T = 60\,\mathrm{ms}$$

from a remote, Linux-based, PC. The camera is mounted on a Windows-based PC where an estimation algorithm runs at a sampling time of $50\,\mathrm{ms}$ and communicates with the Linux-PC via the UDP/IP protocol. Due to the stochastic nature of the communications, a small phenomenon of random sampling is to be expected.

The robot is moved using a simple via-point navigation algorithm. At the initial time the robot is simply put somewhere in the arena. The trajectory is $100\,\mathrm{s}$ long.

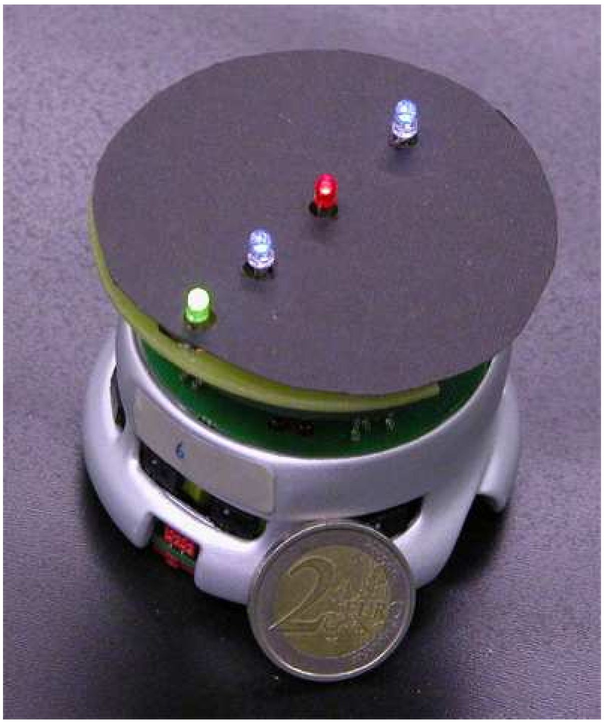

Fig. 2. The Khepera II mobile robot.

The proposed filter were compared with the EKF based on [14]. To emulate a multi-rate working condition, both the filters use the encoder readings at T and the vision data at a sample time of

$$T_v = 10 \cdot T = 600\,\mathrm{ms}$$

and use the temporal update in between those samples. In the proposed filter, the temporal update is achieved by running the equations (15) with null gains.

Since the vision data is stored at the smaller sample time of T, for evaluation purposes the errors are computed using this sample time.

A. Discretized filter

The filter's equations presented in eq. (10) were implemented in the following discrete-time version:

$$\begin{cases} \hat{\boldsymbol{p}}(k+1) = \hat{\boldsymbol{p}}(k) + \boldsymbol{\Phi}(k)\hat{\boldsymbol{\beta}}(k) + \boldsymbol{K}_{p}\tilde{\boldsymbol{p}}(k) \\ \hat{\boldsymbol{\beta}}(k+1) = \hat{\boldsymbol{\beta}}(k) + \boldsymbol{K}_{\beta}\boldsymbol{\Phi}(k)^{\mathrm{T}}\tilde{\boldsymbol{p}}(k)\,, \end{cases} \tag{15}$$

where k denotes the sample time.

B. EKF equations

The experimental comparison were made with respect to the well known Extended Kalman Filter. The implemented version is similar to the one presented in [14] with the sole difference that here the wheels velocities instead of the wheels encoders are used as input for the equations. Let us define as filter's state the vector:

$$\boldsymbol{x} = [\, x \quad y \quad \theta \quad r_L \quad r_R \quad b\,]^{\mathrm{T}} \tag{16}$$

and model the odometry in discrete-time as

$$\begin{aligned} \boldsymbol{x}(k{+}1) &= \boldsymbol{f}(\boldsymbol{x}(k), \omega_R(k), \omega_L(k), \boldsymbol{R}_v) \\ \boldsymbol{z}(k) &= \boldsymbol{H}\boldsymbol{x}(k) + \boldsymbol{R}_w \,, \end{aligned} \tag{17}$$

where $\boldsymbol{f}$ is the nonlinear function that collects the discrete-time version of (1) plus a random walk model for the odometric parameters, $\boldsymbol{R}_v \in \mathbb{R}^{6\times 6}$ represents the process noise, $\boldsymbol{R}_w \in \mathbb{R}^{3\times 3}$ represents the measurement noise, while the output matrix $\boldsymbol{H} \in \mathbb{R}^{3\times 6}$ is constant and defined as

$$\boldsymbol{H} = [\, \boldsymbol{I}_3 \quad \boldsymbol{O}_3\,] \tag{18}$$

where $\boldsymbol{I}_3$ is the 3×3 Identity matrix and $\boldsymbol{O}_3$ is a null 3×3 matrix. The classic EKF equations are used, in details:

$$\begin{aligned} \boldsymbol{L} &= \boldsymbol{M}\boldsymbol{H}^{\mathrm{T}} \left(\boldsymbol{R}_v + \boldsymbol{H}\boldsymbol{M}\boldsymbol{H}^{\mathrm{T}}\right)^{-1} \\ \boldsymbol{x}(k)^{(+)} &= \boldsymbol{x}(k)^{(-)} + \boldsymbol{L}\left(\boldsymbol{z}(k) - \boldsymbol{H}\boldsymbol{x}(k)^{(-)}\right) \\ \boldsymbol{P} &= \boldsymbol{M} - \boldsymbol{M}\boldsymbol{H}^{\mathrm{T}} \left(\boldsymbol{R}_v + \boldsymbol{H}\boldsymbol{M}\boldsymbol{H}^{\mathrm{T}}\right)^{-1} \boldsymbol{H}\boldsymbol{M} \end{aligned}$$

for the measurement update and

$$\begin{aligned} \boldsymbol{x}(k{+}1)^{(-)} &= \boldsymbol{f}(\boldsymbol{x}(k)^{(+)}, \omega_R(k), \omega_L(k)) \\ \boldsymbol{M} &= \boldsymbol{F}\boldsymbol{P}\boldsymbol{F}^{\mathrm{T}} + \boldsymbol{R}_w \end{aligned}$$

for the temporal update; the linearized extended system matrix $\boldsymbol{F}$ is given by:

$$\boldsymbol{F} = \begin{bmatrix} 1 & 0 & F_{1,3} & F_{1,4} & F_{1,5} & 0 \\ 0 & 1 & F_{2,3} & F_{2,4} & F_{2,5} & 0 \\ 0 & 0 & 1 & F_{3,4} & F_{3,5} & F_{3,6} \\ 0 & 0 & 0 & 1 & 0 & 0 \\ 0 & 0 & 0 & 0 & 1 & 0 \\ 0 & 0 & 0 & 0 & 0 & 1 \end{bmatrix} \tag{19}$$

with

$$\begin{aligned} F_{1,3} &= -\frac{1}{2}T(x_4\omega_L + x_5\omega_R)\sin(x_3) \\ F_{1,4} &= \frac{1}{2}T\omega_L\cos(x_3) \\ F_{1,5} &= \frac{1}{2}T\omega_R\cos(x_3) \\ F_{2,3} &= \frac{1}{2}T(x_4\omega_L + x_5\omega_R)\cos(x_3) \\ F_{2,4} &= \frac{1}{2}T\omega_L\sin(x_3) \\ F_{2,5} &= \frac{1}{2}T\omega_R\sin(x_3) \\ F_{3,4} &= -T\frac{\omega_L}{x_6} \\ F_{3,5} &= T\frac{\omega_R}{x_6} \\ F_{3,6} &= T\frac{x_4\omega_L - x_5\omega_R}{x_6}\,. \end{aligned}$$

C. Gain selection and initialization

Selection of the matrix gains is a critical aspect in making a comparison between two different approaches. In particular, the proposed filter is linear in the parameters while the EKF is non-linear. Moreover, selecting as diagonal all the matrix gains leads to select 7 scalar values for the proposed approach while 9 scalar values for the EKF corresponding to the covariance matrices; however, it is known in the literature that only the *ratio*, in a wide sense, between those matrices influences the EKF's behavior. Finally, the initial value for the Kalman gain $\boldsymbol{M}$ too needs to be selected. Any effort to chose the gains so as to ensure *similar* performance to the filters were made; nevertheless, this is impossible in a strict sense. For this reason, the presented results have to be interpreted mainly looking at the error behavior rather then focusing on direct numeric comparison. In detail, the gains used for the experiments are:

$$\begin{aligned} \boldsymbol{K}_p &= \boldsymbol{I}_3 \\ \boldsymbol{K}_\beta &= 0.05\boldsymbol{I}_4 \\ \boldsymbol{R}_v &= 100\boldsymbol{I}_3 \\ \boldsymbol{R}_w &= \mathrm{diag}\,[\,10 \quad 10 \quad 10 \quad 0.005 \quad 0.005 \quad 10\,] \\ \boldsymbol{M} &= \boldsymbol{I}_6 \end{aligned}$$

Based on a CAD value, the initial estimation are based on the nominal values of

$$\begin{aligned} r_{L,\text{nominal}} &= 0.8\,\text{cm} \\ r_{R,\text{nominal}} &= 0.8\,\text{cm} \\ b_{\text{nominal}} &= 5.333\,\text{cm} \end{aligned}$$

and correspond to

$$\begin{aligned} \hat{\boldsymbol{\beta}}(k{=}0) &= [\,0.8 \quad 0.8 \quad 0.15 \quad 0.15\,]^{\mathrm{T}} \\ \hat{\boldsymbol{x}}(k{=}0) &= [\,\hat{x}(0) \quad \hat{y}(0) \quad \hat{\theta}(0) \quad 0.8 \quad 0.8 \quad 5.333\,]^{\mathrm{T}} \end{aligned}$$

where the initial robot configuration is taken as the first measured value.

D. Experimental results

Figure 3 shows the path performed by the vehicle, notice that the data used to evaluate the filters are the same used in [2], [3] to perform off-line estimation of the physical odometric parameters, a comment about will follow. The motion of the vehicle is achieved using a simple via-point guidance algorithm.

Figures 4 and 5 show the values of the estimated parameters using the proposed filter, please notice that the variables in figure 5 are a-dimensional.

Figure 6 shows the value of β_1 and β_2 estimated with the proposed together with the corresponding value r_R and r_L estimated with the EKF approach. The filters output numerically similar values and, due to a proper selection of the gains, also with a similar dynamics.

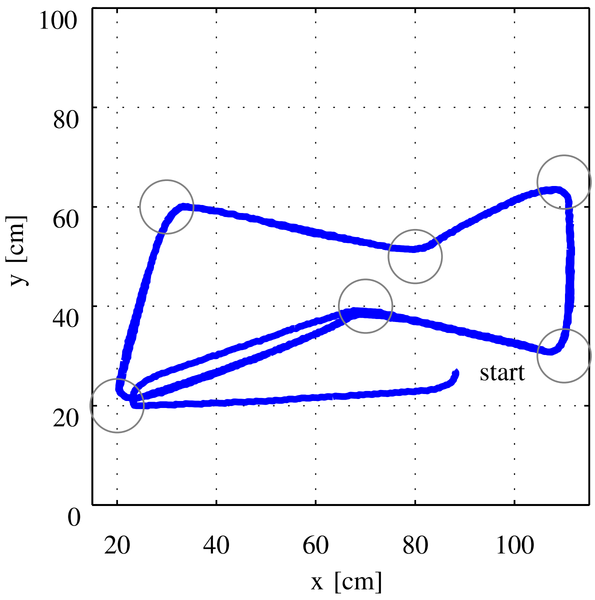

Fig. 3. Path performed by the vehicle.

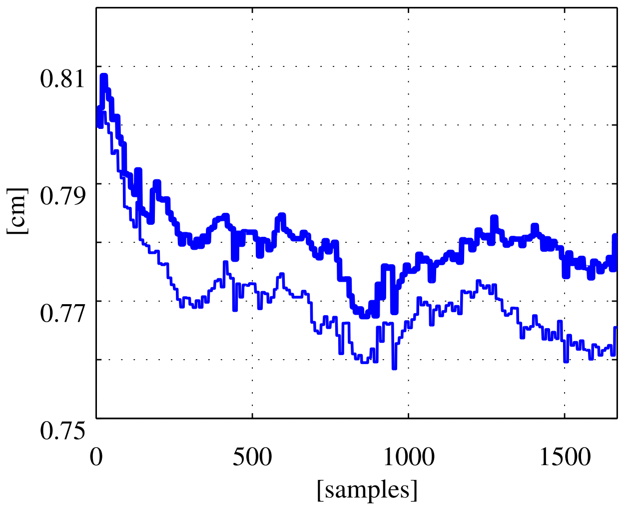

Fig. 4. Estimated value of β_1 (thick line) and β_2 (thin line) during the motion.

Figure 7 shows the value of $\hat{b}$ where some numerical differences can be appreciated. It should be noted, however, that the proposed filter is based on a 4-parameters set of unknowns that guarantee a linear relationship with the data and not on the physical parameters as the EKF. For that reason, the comparison between the $\hat{b}$'s is only indicative.

A measure of the validity of the approaches might be given by the numerical reconstruction errors. Those, however, are close to the resolution of the measurement system ($\approx 0.2\,\mathrm{cm}$) for both filters for the whole trajectory duration. The only conclusion that can be made is that both filters have similar, and good, performance.

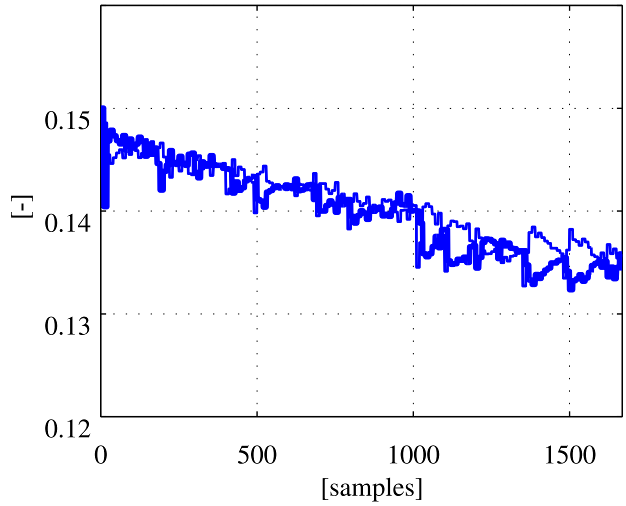

Fig. 5. Estimated value of $-\beta_3$ (thick line) and β_4 (thin line) during the motion.

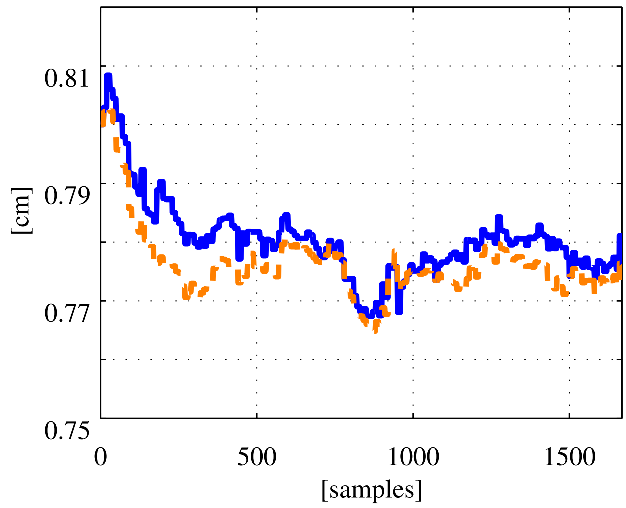

Fig. 6. Estimated value of β_1 (r_L) during the motion: solid-thick-blue line, proposed approach; dashed-thick-orange line, EKF.

E. On-line compared with off-line odometry calibration

In [2], [3], the same data are used to make an off-line estimation of both the physical parameters and the vector $\boldsymbol{\beta}$. It is worth noticing the difference between the algorithms. The identification procedure in [2], [3] is made off-line, since a linear relationship arises between unknown and data the estimation converges to the true value. In the proposed approach, and in any on-line adaptive algorithm, it is not guaranteed that the estimation converges to the true value but only that the error is limited. Concerning the EKF, however, no formal proof of convergence exists.

V. Conclusions

In this paper, a deterministic filter to localize the vehicle while estimating a proper set of odometric parameters is

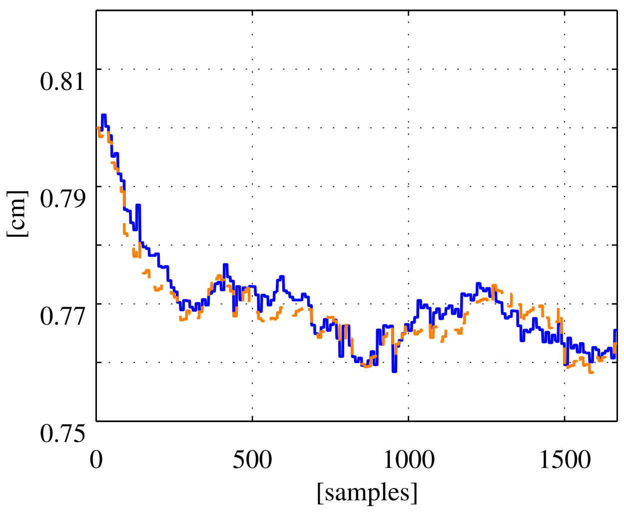

Fig. 7. Estimated value of β_2 (r_R) during the motion: solid-thin-blue line, proposed approach; dashed-thin-orange line, EKF.

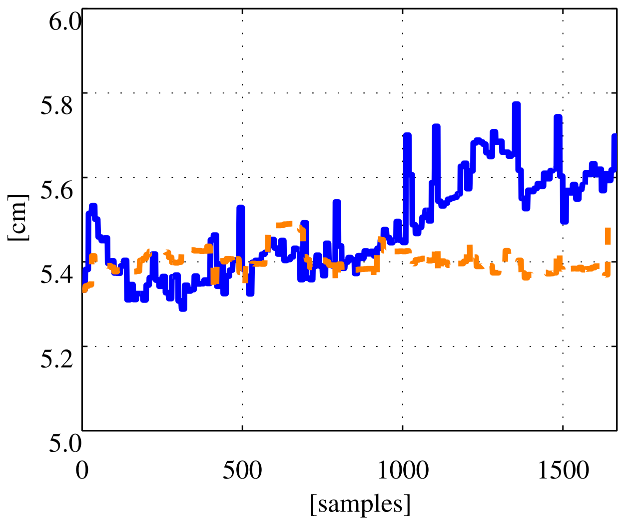

Fig. 8. Estimated value of $\hat{b}$ during the motion: solid-blue line, proposed approach; dashed-orange line, EKF.

proposed. A stability analysis is provided that guarantees that the position and orientation error decreases to zero and the estimation error of the odometric parameters is bounded. The proposed technique has been experimentally validated on a Khepera II mobile robot and compared to an Extended Kalman Filter approach. The performance of the algorithms is practically the same. The proposed approach, thus, represents a simpler alternative to the Extended Kalman Filter approach that, in addition, exhibits a rigorous stability analysis.

References

[1] `http://www.k-team.com/`. K-Team.

[2] G. Antonelli and S. Chiaverini. Linear estimation of the odometric parameters for differential-drive mobile robots. In *2006 IEEE/RSJ International Conference on Intelligent Robots and Systems*, pages 3287–3292, Beijing, PRC, Oct. 2006.

[3] G. Antonelli and S. Chiaverini. Linear estimation of the physical odometric parameters for differential-drive mobile robots. *accepted Autonomous Robots*, 2007.

[4] G. Antonelli, S. Chiaverini, and G. Fusco. A systematic calibration method for odometry of mobile robots based on the least-squares technique: theory and experimental validation. *IEEE Transactions on Robotics*, 21(5):994–1004, Oct. 2005.

[5] P. Bonnifait, P. Bouron, P. Croubillé, and D. Meizel. Data fusion of four ABS sensors and GPS for an enhanced localization of car-like vehicles. In *Proceedings 2001 IEEE International Conference on Robotics and Automation*, pages 1597–1602, Seoul, KR, May 2001.

[6] J. Borenstein and L. Feng. Measurement and correction of systematic odometry errors in mobile robots. *IEEE Transactions on Robotics and Automation*, 12(6):869–880, 1996.

[7] D. Caltabiano, G. Muscato, and F. Russo. Localization and self calibration of a robot for volcano exploration. In *Proceedings 2004 IEEE International Conference on Robotics and Automation*, pages 586–591, New Orleans, LA, April 2004.

[8] N.L. Doh, H. Choset, and W.K. Chung. Relative localization using path odometry information. *Autonomous Robots*, June 2006.

[9] P. Goel, S.I. Roumeliotis, and G.S. Sukhatme. Robust localization using relative and absolute position estimates. In *Proceedings 1999 IEEE/RSJ International Conference on Intelligent Robots and Systems*, pages 1134–1140, Kyongju, KR, Oct. 1999.

[10] A. Kelly. General solution for linearized systematic error propagation in vehicle odometry. In *Proceedings 2001 IEEE/RSJ International Conference on Intelligent Robots and Systems*, pages 1938–1945, Maui, HI, Nov. 2001.

[11] A. Kelly. General solution for linearized stochastic error propagation in vehicle odometry. In *Preprints 15th IFAC World Congress*, Barcelona, Spain, July 2002.

[12] H.K. Khalil. *Nonlinear Systems*. Prentice-Hall, Upper Saddle River, New Jersey, 2nd edition, 1996.

[13] K. Komoriya and E. Oyama. Position estimation of a mobile robot using optical fiber gyroscope (OFG). In *Proceedings 1994 IEEE/RSJ International Conference on Intelligent Robots and System*, pages 143–149, Munich, D, Sept. 1994.

[14] T.D. Larsen, M. Bak, N.A. Andersen, and O. Ravn. Location estimation for autonomously guided vehicle using an augmented Kalman filter to autocalibrate the odometry. In *Proceedings FUSION98 Spie Conference*, Las Vegas, NE, July 1998.

[15] A. Martinelli, N. Tomatis, A. Tapus, and R. Siegwart. Simultaneous localization and odometry calibration. In *Proceedings IEEE/RSJ International Conference on Intelligent Robots and Systems*, pages 1499–1504, Las Vegas, NE, Oct. 2003.

[16] N. Roy and S. Thrun. Online self-calibration for mobile robots. In *Proceedings 1999 IEEE International Conference on Robotics and Automation*, pages 2292–2297, Detroit, MI, May 1999.

[17] C.M. Wang. Location estimation and uncertainty analysis for mobile robots. In *Proceedings 1988 IEEE International Conference on Robotics and Automation*, pages 1230–1235, Philadelphia, PA, 1988.